Robust PID Control in Chemical Process Industries

Rakesh Joshi[1], Kostas Tsakalis[1], J. Ward MacArthur[2], Sachi Dash[3]

Abstract

Robust control design has been increasingly used in industrial settings by leading automation companies. The design procedure has evolved in the last decades and fairly automated procedures exist now for use by practicing engineers or even operators. One does not need to be familiar with the details of the underlying theory to use it. Robust control is different than conventional control in that it accounts for uncertainty bounds and designs a controller with known/desired performance and stability characteristics. Robust control can be applied to multivariable or Single Input Single Output (SISO) processes. This paper is aimed at providing a tutorial on the Robust PID control design approach to practicing chemical engineers. We use the classical pH control problem as an example, which is a challenging problem due to its non-linearity. First, we analyze the pH process by using the benchmark model of Henson and Seborg. We identify the fundamental limitations of the linear control design in terms of model uncertainty and sensor sampling constraints. Subsequently, we design a controller following the guidelines from robust control theory. Finally, we demonstrate the results though implementation in a lab-scale wastewater system. The experimental results show the validity of the process model and the control design approach. It also points out the limitations of the linear controller performance, leading to an interesting follow-up work regarding gain scheduling and adaptation.

Introduction

Control theory provides a solid base for designing controllers for the industrial processes. An engineer who is designing controllers should make sure that the designed controllers produce a stable closed-loop and satisfy given closed-loop specifications. Some of the important closed-loop specifications are the time constant and allowable percent overshoot. Most of the controller design methods require a linear model (nominal model) of the process. Frequency domain dominates the analysis in modern techniques, although more recent methods can be used to formulate time and frequency domain specifications in convex optimization objectives. Controller specifications listed above can be translated into closed-loop bandwidth (roughly the inverse of the closed-loop time constant) and the peak of the closed-loop frequency response.

The nominal model response can deviate from the actual response due to a variety of factors, such as the presence of nonlinearity, noise, and unmodeled dynamics. The term "uncertainty" in robust control theory refers to the differences between the model (nominal) response and true process response. There are many ways of describing uncertainty. The robust control theory helps practicing engineers to design controllers for the nominal model with uncertainty so that the closed-loop system remains stable and has the specified performance regardless of the exact properties of the actual process.

This paper describes a procedure for the analysis of a dynamical system or plant for the purposes of feedback control and robust PID design. This procedure is illustrated by using two examples, one with a first-principles model (from physical laws like mass balance and charge balance) and one with an experimental process model (where the model is directly determined from fitting experimental data), bringing out their similarities and differences. Lastly, limitations of linear controllers motivate the need for nonlinear controller design and some specific solutions are discussed.

The procedure for system analysis and robust controller design used in the process industry is summarized in the Figure 1. It should of course be understood that not all steps are explicitly followed in every case nor are they given equal weight. The basic steps are as follows:

- **Understand the process and the control requirements:** It is important to understand the dynamic process behavior near an operating point, for example by looking at the speed and directionality of the step response of the actual process or simulation of its approximate model. Some important aspects are process variables

1 Arizona State University, School of Electrical Computer and Energy Engineering; AZ; 2&3 Honeywell International; 3 Corresponding Author

that need to be controlled, acceptable variation from the set point and the magnitude and frequency of the disturbances entering the process. It is also important to understand the limitations imposed by the actuators and sensors. Actuator limitations include dynamics, maximum and minimum limits, hysteresis and other nonlinearities. Typical sensor limitations come from sampling-time constraints, accuracy, and precision or noise characteristics.

- **Model the process and compute uncertainties:** One way of modeling process behavior is using first-principles like mass balance, charge balance and energy balance. This method allows for a deeper process understanding at the nominal operating point, but also away from it. It is very complex and time consuming and it is not always clear what level of detail is needed for controller design purposes. Another way of obtaining a process model (such as, a Laplace transfer function) is by performing identification experiments. This involves performing experiments by exciting the process and using the recorded input-output time series data to fit the model. There are many packages and tools available in the industry to identify a model from the data. System identification procedures for robust control are described in [5], [6], [7] and [9]. With the recent advances in both theory and computational tools, there is a growing interest towards data driven models which, by design, emphasize only the more important components of the system response, actuator and sensor dynamics, nonlinearities, and accuracy characteristics. The availability of actual data also allows for the computation of realistic estimates of the dynamic uncertainty (this estimate can take many forms, one such form called multiplicative uncertainty, is discussed in the next paragraph), which describes the range of validity of the model and is critical in controller design. On the other hand, such models are not easy to generalize or use for extrapolation purposes, away from the modeled operating conditions. Overall, it is fairly clear that a combination of first-principles modeling (for a suitable model structure and design of experiments) and data-driven modeling (for fine tuning and uncertainty characterization) offers the best promise for the development of a control-relevant model. However, the exact characteristics of each are not easy to determine a priori.

  Uncertainty computation: Understanding dynamic uncertainty of the process model is a very important aspect of robust controller design. There are several ways of characterizing uncertainty and they are not always equivalent. Nevertheless, a conceptually simple and fairly general characterization is in terms of the multiplicative uncertainty (Δ_m), i.e., the percent output error. This error is not necessarily a random variable but may have dynamics, i.e., be itself described by an unknown transfer function (See Appendix: A1 for more details). The interest in this form of uncertainty comes from its interpretation as an upper bound for the closed-loop system bandwidth. More specifically, for the nominal process model (P) and controller (C), the complementary sensitivity T of the closed-loop system is defined as:

$$T = \frac{PC}{1+PC} \qquad \text{Eq. (1)}$$

  According to the small gain theorem, the closed-loop system of the perturbed process model $P(1 + \Delta_m)$ and the controller C will be stable for all stable uncertainty operators that satisfy (See Appendix: A1 for more details):

$$|T(j\omega)||\Delta_m(j\omega)| < 1 \qquad \text{Eq. (2)}$$

  Since in general, the multiplicative uncertainty grows with frequency, this condition implies that the complementary sensitivity should roll-off (become smaller as the frequency becomes large), imposing limitations on the closed-loop bandwidth and hence, speed of response. Alternatively, this can be viewed

as a signal-to-noise ratio (SNR) condition, namely that effective control can occur as long as the SNR (modeled output to output error) is greater than unity.

- **Specify desirable and achievable control objectives:** Time domain specifications for the closed-loop system are closed-loop time constant and percent overshoot in the step set-point change. It is typically desirable to design a closed-loop system that responds fast to set-point changes with minimal overshoot. On the other hand, this may not be achievable due to process delays, inverse response, or process uncertainty. The time constant of a closed-loop specification can be related to the closed-loop bandwidth in the frequency domain (approximately, the inverse of the closed-loop time constant). The choice of closed-loop bandwidth for the controller design is the single most important specification for the controller design as it directly corresponds to the speed of the closed-loop response. It is also a very convenient design parameter since it is easily manipulated during the computation of the controller parameters. The achievable closed-loop bandwidth (theoretical limit) and percent overshoot are affected by the uncertainty, sampling time of sensor and other delays in general, model characteristics like instability of the process model, transportation delays and sensor noise. Overall, the closed-loop specifications can be defined in terms of a "target loop", which should then be approximated by the closed-loop with the designed controller. This problem is typically easier to solve computationally in the general case, than a generic bandwidth or overshoot specification. The relationship between process model characteristics like transportation delays, inverse responses and instability and the choice of a "target loop" in controller design has been a subject of considerable analysis [3], while some guidelines target loop selection can be found in [8].
- **Compute the controller parameters:** For the given controller specifications, there is a variety of sophisticated linear and nonlinear controllers available both in theory and in industrial applications. However, proportional-integral-derivative (PID) controllers are the most common with industrial usage up to 95%. There are many procedures available for tuning PID gains like Ziegler-Nichols, Internal Model Control (IMC) [11], or optimization-based and, when used appropriately, they work as well as any other [9]. The more substantial advantages of one method over another are typically in minimizing design iterations, clarity of requirements from the modeling and data collection steps, ease of use and training. The choice of design procedure is not important, as long as the designed controller satisfies a robust stability condition imposed by uncertainty (see Appendix: A1). A PID controller design using frequency loop shaping is used in this paper. In this method PID parameters are tuned to achieve loop transfer function close to the chosen "target loop", where the choice of a target loop, the procedure for tuning PID and its limitations are described in more detail in [8].
- **Validate the closed-loop control system:** The designed controller is validated in the frequency domain and in the time domain using simulations. The frequency domain validation includes verification of the small gain robust stability condition for the model uncertainty (See Appendix: A1 for details). The designed controller is validated in the time domain by analyzing the step responses of the closed-loop system to set-point changes and disturbances. Depending on the severity of nonlinearities in actuators and sensors, the designer should also evaluate in this step the effect of saturating actuators, sensor sampling delays, noise and quantization. For example, an iteration may be necessary if the observed noise is too large and causes excessive movement in the actuators.
- **Implement and test the closed-loop control system:** Once the controller is validated, it is implemented and tested on the actual process for set point tracking and disturbance rejection. This step will reveal inconsistencies, if any, between the testing conditions and the actual system operation, in which case a controller redesign, or even a redesign of the excitation conditions for system identification, may be necessary.

pH neutralization model analysis and controller design

Our motivating application is the control of pH at a given desired level (5-9), which is required in wastewater treatment for process optimization. This section focuses on analysis and controller design of the pH neutralization process model described in [1]. The same nominal operating conditions as described in [1] are used for this model. (See Appendix*:* A2 for the brief description of the model). The process model is linearized around pH=6 and pH=8 and, as it turns out, the transfer functions of these models in minutes are represented as follows:

$$P_m(s) = \frac{K}{\tau s+1} \qquad \text{Eq. (3)}$$

The individual parameters for this expression are given in Table 1, where $\mathrm{P_{m6}(s)}$ and $\mathrm{P_{m8}(s)}$ are the transfer functions of linear models at pH = 6 and pH = 8 respectively. The unit step responses of these process models are shown in Figure 2. These plots are used as examples to illustrate the more general observation arising from the analytical study of the first-principles model that both models have similar time-constants but very different steady state gains. This is also verified by examining the step and frequency responses of several other linearized models at intermediate pH values (omitted here for clarity).

To determine the suitability of a single controller to control the process, we consider the performance of a controller designed for one pH value, and evaluate it at all other pH operating points. For example, we choose pH = 6 as the nominal operating point for the controller design and then calculate the multiplicative uncertainty for the model at pH = 8. The plots of multiplicative error provide an estimate of multiplicative uncertainty arising due to changes in the operating conditions. As shown in Figure 2a, with either one as the nominal model, the multiplicative uncertainty is near or greater than unity. This results in robust stability conditions (Eq. 2) that are violated or satisfied with a small margin, implying that a single (linear) controller cannot approximate well a particular closed-loop target. For more detailed models, the uncertainty may also be affected by the inclusion of actuator and sensor dynamics which themselves can be uncertain. To complete this step, a target bandwidth of 0.6rad/min is chosen for controller design based on the sensor sampling constraints (>1sec), actuator capabilities and some trial-and-error. The transfer functions of the designed PI controllers (for this process model a derivative action is not needed) are given below as $C_{m6}(s)$ and $C_{m8}(s)$, which are PI controllers of the linearized process models at pH = 6 and pH = 8 respectively.

$$C_{m6}(s) = 106.53\left(1 + \frac{1}{1.44\,s}\right) \qquad \text{Eq. (4)}$$

$$C_{m8}(s) = 14.20\left(1 + \frac{1}{1.38\,s}\right) \qquad \text{Eq. (5)}$$

The controller C_{m6} fails the frequency domain validation since the value of the uncertainty is higher than one for all frequencies and, even though there is no closed-loop instability, this is manifested by a large variability in the closed-loop responses. Figures 3a and 3b show the step responses of the closed-loop system with controllers $C_{m6}$and C_{m8} respectively. At pH = 6, C_{m6} results in the expected performance (settling time of 8 min), and so does C_{m8} at pH = 8. At pH = 6 response of the closed-loop system with C_{m8} is very slow with settling time around 25 minutes. At pH = 8 the response of the closed-loop system with C_{m6} is very fast with settling time around 1 minute. This is also undesirable since the choice of bandwidth will ultimately depend on uncertainty and robustness considerations and a faster loop may exhibit instability when implemented. On the other hand, the integral time constants are very similar 1.44 for $\mathrm{C_{m6}}$ and 1.38 for $\mathrm{C_{m8}}$, and the difference between the controllers is essentially limited to gain variations, 106.53 for $\mathrm{C_{m6}}$ and 14.20 for $\mathrm{C_{m8}}$. This facilitates the design of a nonlinear (gain-scheduled or adaptive) controller for this process but it extends beyond the scope of this study.

pH control experimental analysis and controller design

This section demonstrates the analysis and controller design procedure using a lab-scale pH control experimental process as an example. First, the experimental setup is discussed in some detail. Second, the system identification results around pH = 5 through 9 are presented. Third, the controller design and choice of bandwidth is discussed. Last, the implementation and validation of these controllers is presented.

The schematic diagram of the experimental setup is shown in Figure 4. The experimental set up consists of a 500ml magnetically stirred reactor with acid, base and buffer flows. The volume inside the reactor is kept constant using an overflow tube. The base flow is used as the control variable, varied by controlling the motor voltage, while the other two flows (acid and buffer) are fixed at 2.45 ml/min.

For the identification of the system model, a Pseudo Random Binary sequence (PRBS) with switching time of 100 sec signal is used as input to Pump 2 to perturb the system around the operating points with pH = 5, 6, 7, 8, and 9. The interest in the two extreme values, which are outside the operating range of the motivating application, is to enable the assessment of the model continuity at the ends of the interval. The output (pH) sequences are measured and then fitted by linear dynamic models. Since the reactor size used in this experiment is 500 ml and the total flow rates (acid + buffer + base) is around 7.35 ml/min, the approximate settling time for the step change in flow is around 3.4 which is 3 times the time constant of the system(3*500/(7.35*60)). Consequently, for the frequency range of interest for our experiments (around 0.6rad/min), the data is expected to be well-represented by an integrating model. The results of the modeling computations are shown in Figure 4 where the step responses of the models at each operating point are plotted. Note that there is an inflection in the rate curve at pH = 7 where the integration rate is lowest, while at pH = 5, 6, 8 and 9 the rate is larger. Also note that the largest gain occurs at a pH = 5.

A small delay is estimated in all models. This delay is attributed to quantization in the sensor and the pump. The quality of the identified models at the various pH levels is shown in Figure 6 in terms of model predictions. This figure shows the measured value of the pH along with the value predicted by the model for a sequence of steps in the base flow rate, which is the input of the process. The output of the model is the predicted value. The transfer functions of the identified models at pH = 6, pH = 7 and pH = 8 have the form given by Eq. (6).

$$P(s) = \frac{K(\tau_1 s+1)}{s(\tau_2 s+1)} e^{-T_d s} \qquad \text{Eq. (6)}$$

The parameters of the various models appear in Table 2, with P_6, P_7 and P_8 denoting the identified model at the corresponding operating point of pH of 6, 7 and 8 respectively. It is worth noting that the experimental results are in line with the results of the linearization of the detailed model presented in [1], showing a large variation of process gain (K) which here is the integration rate.

Next, the uncertainty analysis is performed by examining the spectral power ratio of the residuals to the output which gives an indication of the expected noise to signal ratio in the frequency domain. (A variety of spectral methods can be used for this, but since the interest is just in the uncertainty bound, the results are typically very similar.) Figure 7 shows the inverse of the multiplicative uncertainty estimate, which serves as an upper bound on the loop complementary sensitivity which, in turn, provides an upper bound on the controller gains. It is quite clear that for the robust stability condition to be satisfied, the loop should have bandwidth less than 1rad/min. This is the point that the inverse multiplicative uncertainty becomes unity, as shown in the figure. At higher frequencies the value becomes less than one which indicates that the controller should be attenuating the loop signals.

Based on the uncertainty estimate, a loop bandwidth of 0.6 rad/min is chosen for the controller design for the both process models (pH = 6 and pH = 8) as it satisfies robustness with some margin, sampling time constraints, and is consistent with actuator saturation limits and quantization noise levels (the last one is verified after a few loop simulations which not shown here). Two controllers are designed, one at pH=6 and the other at pH=8. The closed-loop systems are tested at nominal and off-nominal conditions. The term “nominal condition” refers to the point at which the controller was designed to operate. The transfer functions of the two controllers are:

$$\mathrm{C}_6(\mathrm{s}) = 12450\left(1 + \frac{1}{2.94\ \mathrm{s}}\right) \qquad \text{Eq. (7)}$$

$$C_8(s) = 3596\left(1 + \frac{1}{2.36\ s}\right) \qquad \text{Eq. (8)}$$

Both controllers satisfy the small gain theorem for the respective model uncertainty characterization and provide reasonable responses during a simulation-based validation. Figure 8a shows the experimentally measured step responses of closed-loop system with the controllers C_6 and C_8 at their respective nominal pH conditions. These agree very well with the simulated closed-loop responses, something that verifies the success of the identification process. Figures 8b & c compare the closed-loop responses with the controller for the alternative operating point (off-nominal design). The performance degrades by either becoming too slow, or too fast, which in some cases can also result in oscillatory behavior or instability. Figure 9 shows one such extreme case where the closed-loop system is destabilized when the C_6 controller operates near pH = 4.5 where the process gain is high.

Discussion and conclusions

The pH control problem exhibits several interesting characteristics that are associated with the process nonlinearity and the uncertainty (or complexity) in the description of the practical components, such as sensors and actuators. The process itself undergoes large gain variations, which means that simple controllers, such as a standard PI/PID, would either require significant performance compromises, or restriction of their operation to a tight range. The paper provided a brief overview of a complete controller design procedure, starting with first principles and data and ending with controller validation. The experimental results show that, in the vicinity of an operating point, the process model and its limitations of achievable performance can be identified with confidence, and a controller can be designed to achieve them by means of a systematic procedure. On the other hand, there is significant performance degradation in pH control when operating away from the nominal design conditions. Performance degradation can be expected due to the nonlinear behavior of the process or other changes in the process parameters, and becomes more pronounced as the process moves further away from its nominal operating conditions.

This raises the important question whether control performance can be improved in a wider range of operation by online controller scheduling or adaptation. Based on preliminary work, beyond the scope of this text, we expect that uniform performance can be achieved by using more sophisticated, nonlinear controller schemes. For example, the Nonlinear Model Predictive Controller paradigm can be followed, whereby the Control input is chosen based on the identification full nonlinear process models, e.g., the Hammerstein model, such that it minimizes a suitable error (e.g., set-point tracking) for a given prediction horizon. Details of this method can be found in [10]. A different approach would be to invoke the general principle of Gain Scheduling and design different controllers for different operating points and schedule them based on independent measurements that determine the operating point. Alternatively, one can also apply adaptive control principles to estimate the controller gains based on input-output measurements. Such an adaptive PID is of particular interest here, since the controller complexity is kept low, while the effective variability can be attributed to a single parameter which can be estimated reliably with very modest excitation requirements. Details of this method are found in [4] and an application to the pH problem will be the subject of a future study.

Acknowledgements

The authors acknowledge the financial support from SERDP Environmental Restoration Projects #2237 and #2239. Special thanks to Professor Amy Childress (University of Southern California), Professor Cesar Torres and Dr. Sudeep Popat (Arizona State University) and Professor Eric Marchand (University of Nevada, Reno) for their valuable input in identifying the specific issues with pH control in the Wastewater System.

References

[1] Henson, M.A.; Seborg, D.E., "Adaptive nonlinear control of a pH neutralization process," Control Systems Technology, IEEE Transactions on , vol.2, no.3, pp.169,182, Sep 1994.

[2] K. Zhou, J.C. Doyle, and K. Glover, "Robust and Optimal Control," . Englewood Cliffs, NJ: Prentice Hall, 1996.

[3] J. C. Doyle, B. Francis, A. Tannenbaum, "Feedback Control Theory," MacMillan, 1992.
[4] Tsakalis, Kostas, Dash, Sachi, "Approximate H∞ loop shaping in PID parameter adaptation," Int. J. Adapt. Control Signal Process, vol. 27, issue 1-2, 2013.
[5] Lennart Ljung "System Identification - Theory For the User," 2nd edition, PTR Prentice Hall, Upper Saddle River, N.J., 1999.
[6] Zhan, C.Q.; Tsakalis, K., "System Identification for Robust Control," American Control Conference, 2007. ACC '07, vol., no., pp.846,851, 9-13 July 2007.
[7] Hernán Alvarez,*, Carlos Londoño,Fernando di Sciascio, and, and Ricardo Carelli , " pH Neutralization Process as a Benchmark for Testing Nonlinear Controllers," Industrial & Engineering Chemistry Research 2001 *40* (11), 2467-2473.
[8] Grassi, E.; Tsakalis, Kostas S.; Dash, S.; Gaikwad, S.V.; MacArthur, W.; Stein, G., "Integrated system identification and PID controller tuning by frequency loop-shaping," Control Systems Technology, IEEE Transactions on , vol.9, no.2, pp.285,294, Mar 2001.
[9] Karl J. Åström. and K. J. Hagglund, " PID controllers : theory, design, and tuning," Research Triangle Park, NC: Instrument Society of America, 1995.
[10] J. Ward MacArthur, "A new approach for nonlinear process identification using orthonormal bases and ordinal splines ", Journal of Process Control, 22 (2012) 375– 389.
[11 Rivera, Daniel E. and Morari, Manfred and Skogestad, Sigurd, "Internal model control: PID controller design" Industrial & Engineering Chemistry Process Design and Development 1986 25 (1), 252-265.
[12] S. Skogestad and I. Postlethwaite , "Multivariable Feedback Control: Analysis and Design" ,Wiley, Chichester, U.K., 1996.
[13] Morari, M. and Zafiriou, E., "Robust Process Control", Prentice Hall, 1989.

Appendix

A1: Robust control framework description

This section provides a brief description of the key concepts of robust control theory, with references [1], [12] and [13] providing an excellent background. First, the multiplicative uncertainty is introduced to characterize and quantify the modeling error. Second, the small gain theorem is stated which is a cornerstone of connecting controller design with modeling uncertainty. In particular, its application to the case of multiplicative uncertainty yields a fairly intuitive approach to robust control.

Multiplicative uncertainty

The multiplicative uncertainty describes the mismatch between the actual process and its model in a normalized sense. Let P be an actual process between the input (u) and the output (y) and let P_0 be the nominal process model. Then the multiplicative uncertainty (Δ_m) is defined as follows:

$$\Delta_m = \frac{P-P_0}{P_0} \qquad \text{A1. (1)}$$

A block diagram of this description is shown in figure A1:1. For nonlinear systems the multiplicative uncertainty of the process model at a nominal operating point (P_o) can be estimated by computing a bound of the multiplicative differences from the models at different operating points (i.e., using A1.1, with $P = P_i$). This is only an estimate and becomes accurate under quasi-steady-state assumptions but it is useful in establishing the minimum degree of robustness that a controller should possess. The maximum uncertainty associated with the nominal model (P_o) is computed by taking the maximum of the magnitude of the frequency response of the multiplicative uncertainty for all process models (P_i).

In the case of identification of the model form the experiment data, estimation error can be expressed in terms of the multiplicative uncertainty (percent output error). A simple formula for calculating a frequency domain estimate of the multiplicative uncertainty, is as follows:

$$|\Delta_m(j\omega)| = \frac{|FFT(y-y_m)|}{|FFT(y_m)|} \quad \text{A1. (2)}$$

Here, y is the actual output of the identification experiment, y_m is the estimated output from the model; $|\Delta_m(j\omega)|$ denotes the magnitude of multiplicative uncertainty at frequency ω; and FFT refers to Fast-Fourier transform.

Small gain theorem

Consider generalized feedback system shown in the figure A1:2, where, M is a nominal model and Δ is an uncertain system for which a bound is available in terms of the amplitude of its frequency response. Then the feedback system is stable if the following frequency domain condition is true:

$$|\Delta(j\omega)||M(j\omega)| < 1, \ \forall\, \omega. \quad \text{A1. (3)}$$

Here $|\Delta(j\omega)|$ and $|M(j\omega)|$ are magnitudes of the frequency response of the uncertainty (Δ) and the model (M), respectively. The inequality is referred to as a Robust Stability Condition for the feedback system.

Application of Small Gain theorem to Multiplicative Uncertainty

Consider the block diagram shown in figure A1:3 of the closed-loop system with multiplicative uncertainty. Here r is a set-point signal, u and y are the process input and output, respectively. The application of the small gain theorem results in the following robust stability condition

$$|\Delta(j\omega)||T(j\omega)| < 1, \ \forall\, \omega. \quad \text{A1. (4)}$$

Where $|\Delta(j\omega)|$ and $|T(j\omega)|$ are magnitudes of the frequency response of the uncertainty (Δ) and the Complementary Sensitivity (T), respectively, which is defined as follows:

$$T = \frac{P_0 C}{1+P_0 C} \quad \text{A1. (5)}$$

To guarantee robust stability, the controller (C) for the nominal process model (P_0) with a multiplicative uncertainty (Δ_m) should be designed such that the robust stability condition A1.4 is satisfied. Roughly, this condition implies that the closed-loop bandwidth cannot be higher than that of the inverse multiplicative uncertainty and that excessive peaks (resonances) should be avoided. In traditional feedback design, these constraints can be translated to crossover frequency and phase margin specifications; modern tools of robust control synthesis allow a tighter design for the same problem and offer certain optimality characteristics.

A2: pH Neutralization model description

The schematic diagram of the pH neutralization process is shown in figure A2:1 and its modeling approach follows from [1]. The reactor type is a continuous stirred tank reactor (CSTR) and its volume is 2500 *m.l.* Baffles are installed to reduce swirling. Inlet streams consist of q1, q2 and q3, where q1 is a strong acid stream, q2 is a weak acid stream (buffer solution) and q3 is a strong base stream. The pH of the reactor is directly measured by a pH probe. The volume of the reactor is kept constant. It is assumed that perfect mixing occurs in the reactor, the temperature is constant and there is complete solubility of the ions involved. The following reactions are taking place in the reactor

$$H_2CO_2 \longleftrightarrow HCO_2^- + H^+ \quad \text{A2. (1)}$$

$$HCO_2^- \longleftrightarrow CO_2^{2-} + H^+ \quad \text{A2. (2)}$$

$$H_2O \longleftrightarrow OH^- + H^+ \quad \text{A2. (3)}$$

The chemical reactions in the reactor are assumed to be at equilibrium. The equilibrium constants of these reactors are defined as below

$$K_{a1} = \frac{[HCO_2^-][H^+]}{[H_2CO_2]} \quad \text{A2. (4)}$$

$$K_{a2} = \frac{[CO_2^{2-}][H^+]}{[HCO_2^-]} \quad \text{A2. (5)}$$

$$K_w = [H^+][OH^-] \quad \text{A2. (6)}$$

The chemical equilibria are modeled using the concept of reaction invariance [1]. For this system, two reaction invariants are involved for each stream (q1, q2, q3 and q4).

$$W_{ai} = [H^+]_i - [OH^-]_i - [HCO_3^-]_i - 2[CO_3^{2-}]_i \quad \text{A2. (7)}$$

$$W_{bi} = [H_2CO_3]_i + [HCO_3^-]_i + [CO_3^{2-}]_i \quad \text{A2. (8)}$$

The relation between a hydrogen ion concentration and reaction invariants is

$$W_{bi}\frac{K_{a1}/[H^+]+2K_{a1}K_{a2}/[H^+]^2}{1+K_{a1}/[H^+]+K_{a1}K_{a2}/[H^+]^2} + W_{ai} + \frac{K_w}{[H^+]} - [H^+] = 0 \quad \text{A2. (9)}$$

The pH value of the solution is obtained by taking the negative logarithm of the $[H^+]$ ion concentration

$$pH = -\log_{10}([H^+]) \quad \text{A2. (10)}$$

A dynamic process model for the pH neutralization process can be derived from the component material balance for the reaction invariants (W_{a4} & W_{b4}) and the algebraic equation relating the pH and reaction invariants. Nominal operating conditions of the plant are described in Table 3.

$$\frac{d(W_{a4})}{dt} = \frac{1}{V}[q_1(W_{a1} - W_{a4}) + q_2(W_{a2} - W_{a4}) + q_3(W_{a3} - W_{a4})] \quad \text{A2. (11)}$$

$$\frac{d(W_{b4})}{dt} = \frac{1}{V}[q_1(W_{b1} - W_{b4}) + q_2(W_{b2} - W_{b4}) + q_3(W_{b3} - W_{b4})] \quad \text{A2. (12)}$$

$$0 = W_{a4} + 10^{(pH-14)} - 10^{(-pH)} + W_{b4}\frac{(1+2\times10^{(pH-pK_2)})}{(1+10^{(pK1-pH)}+10^{(pH-pK_2)})} \quad \text{A2. (13)}$$

Figures

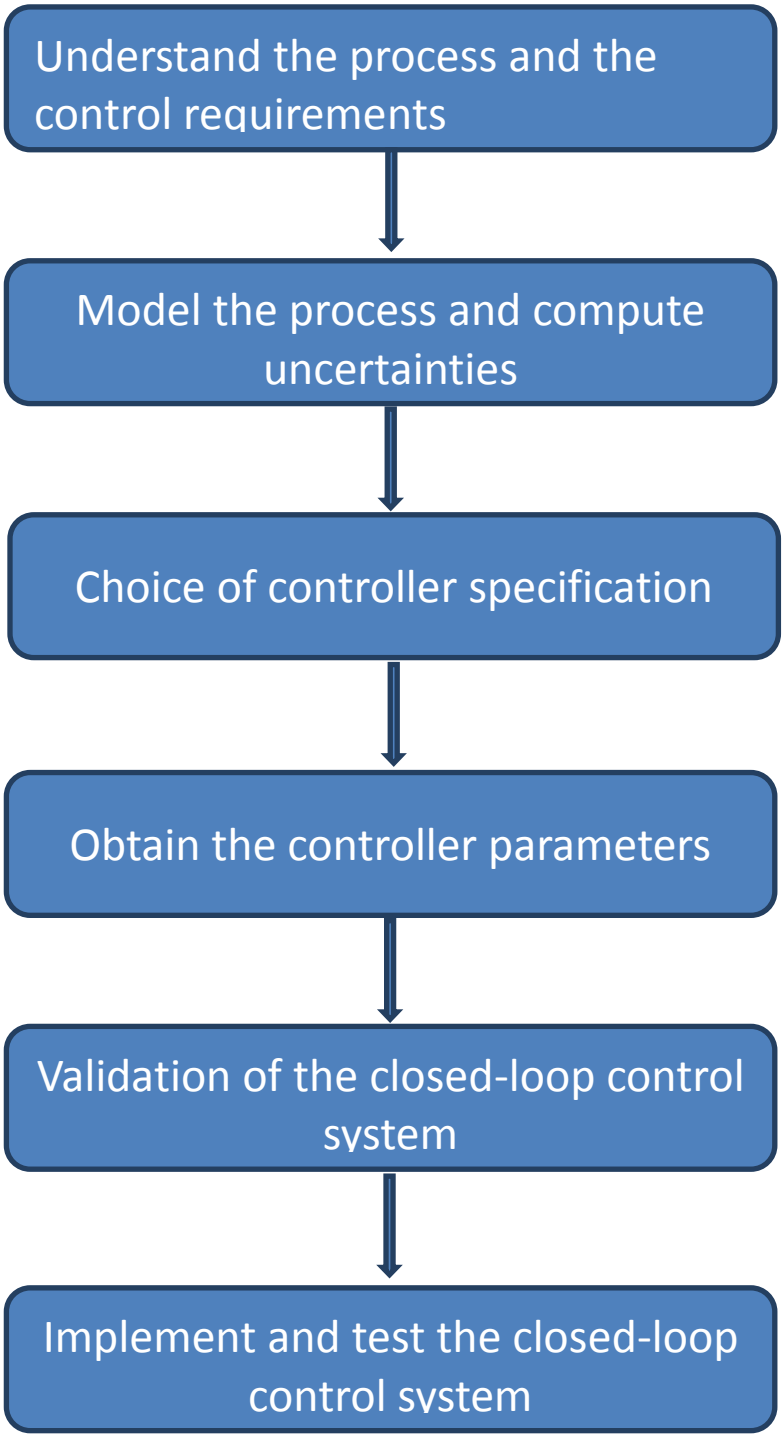

Figure 1 Flow diagram of system analysis and robust controller design procedure

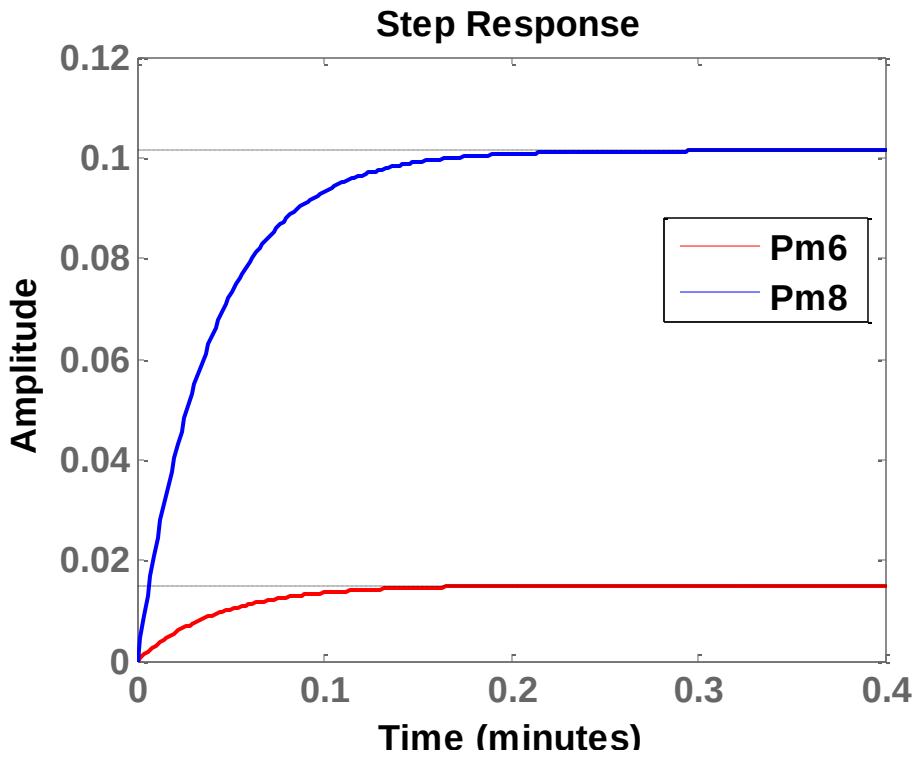

Figure 1. Step responses of linearized models

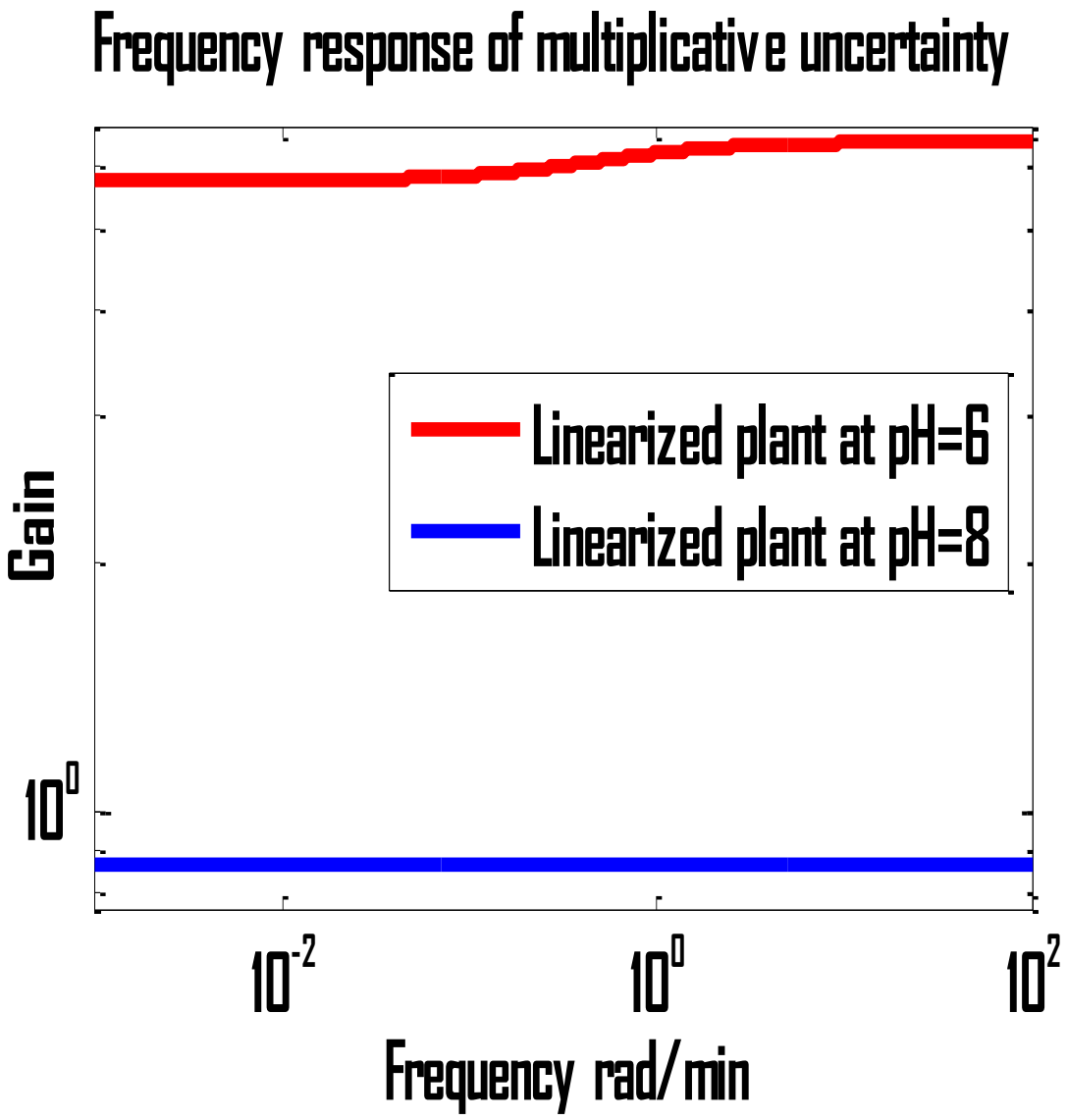

Figure 2. Plots of multiplicative uncertainty

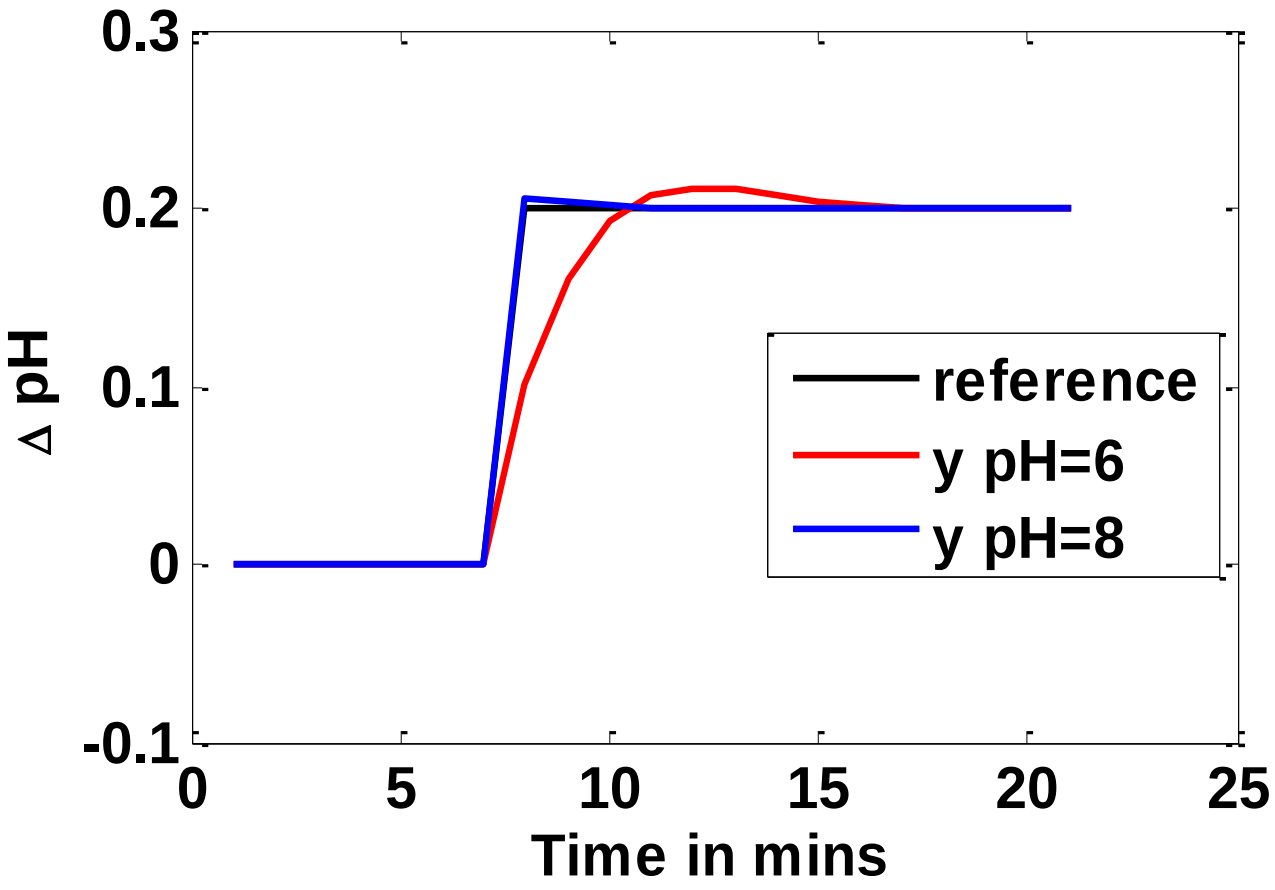

Figure 3a. step responses of Cm_6 controller

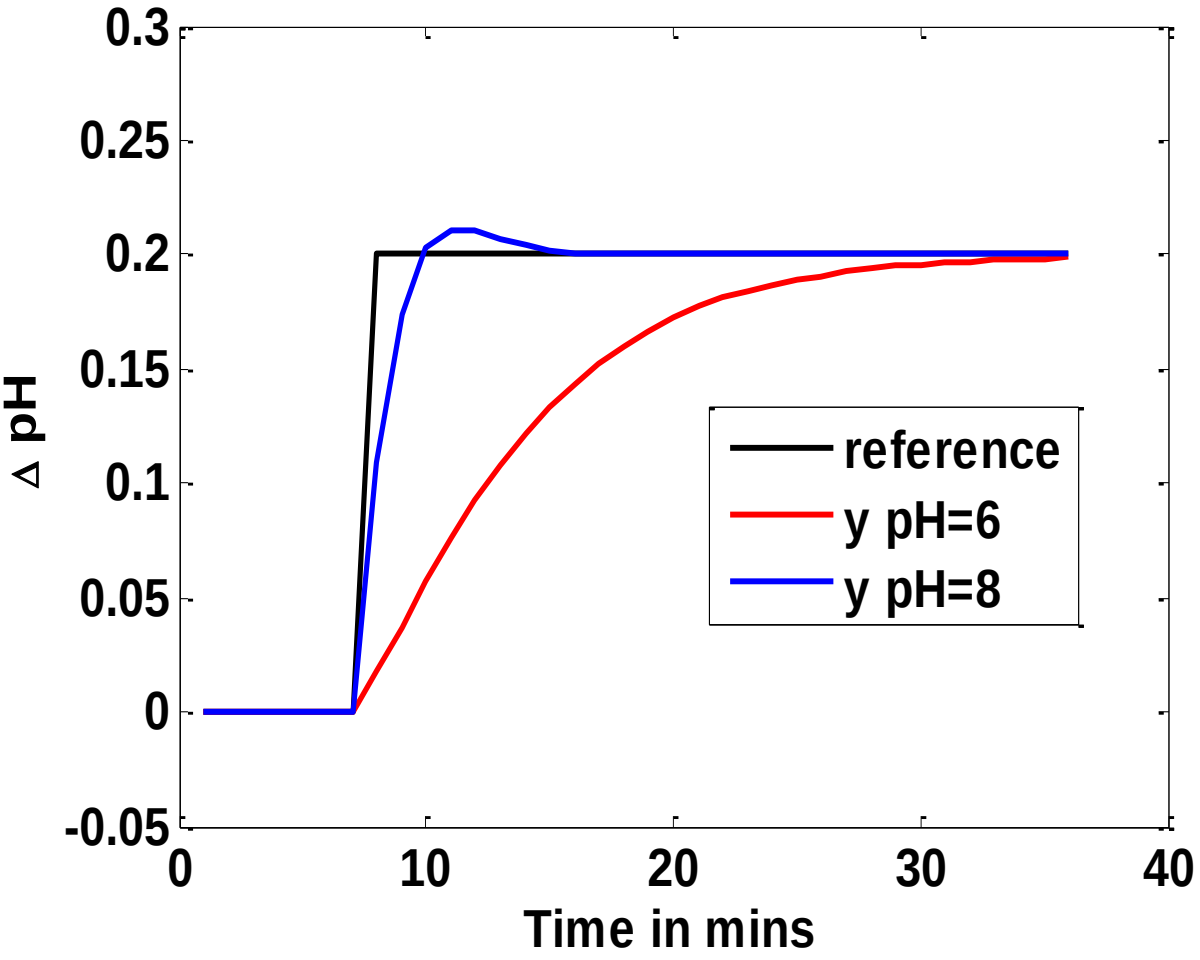

Figure 3b. Sstep responses of Cm_8 controller

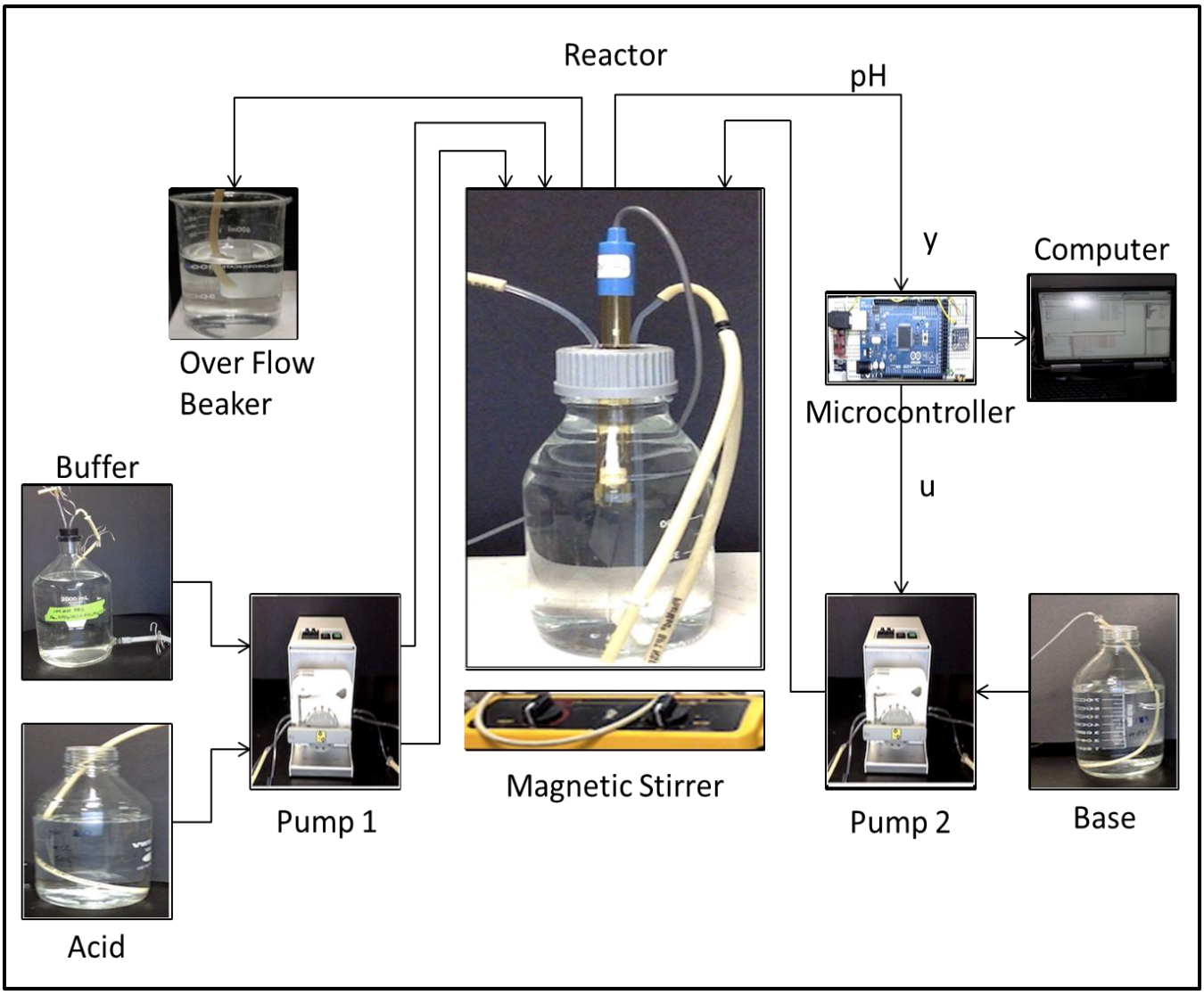

Figure 3a Schematic diagram of Lab scale experimental setup for pH control

Specifications of the experimental setup:

- Reactor size: 500 ml
- Acid: 1 Mol HCl
- Base: 1 Mol NaOH
- Buffer: 100 mMol Phosphate buffered saline
- Pump: Ismatec reglo analog is a peristaltic pump with flow maximum flow rate of 7 ml/min
- Control variable: Voltage across pump (0-5 V)(0-7 ml/min)(0-4095 digital value)
  Base flow $=\frac{(\text{DAC Setpoint})\times 7}{4095}\ ml/min$
- Digital to Analog Converter (DAC): Output range of 0-5 V with 12 bit precision.
- pH Sensor: Atlas Scientific pH sensor with pH circuit 4.0. Maximum sampling rate of 1 second with 95 % accuracy.

Figure 4b, Specifications of the experimental setup

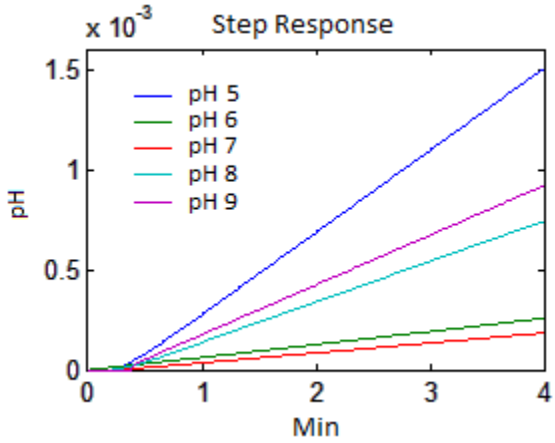

Figure 4, Step responses of all models over 4 minutes

Figure 5, Open-loop Predictions of all models, -green actual output(y) -red predicted output (y_m)

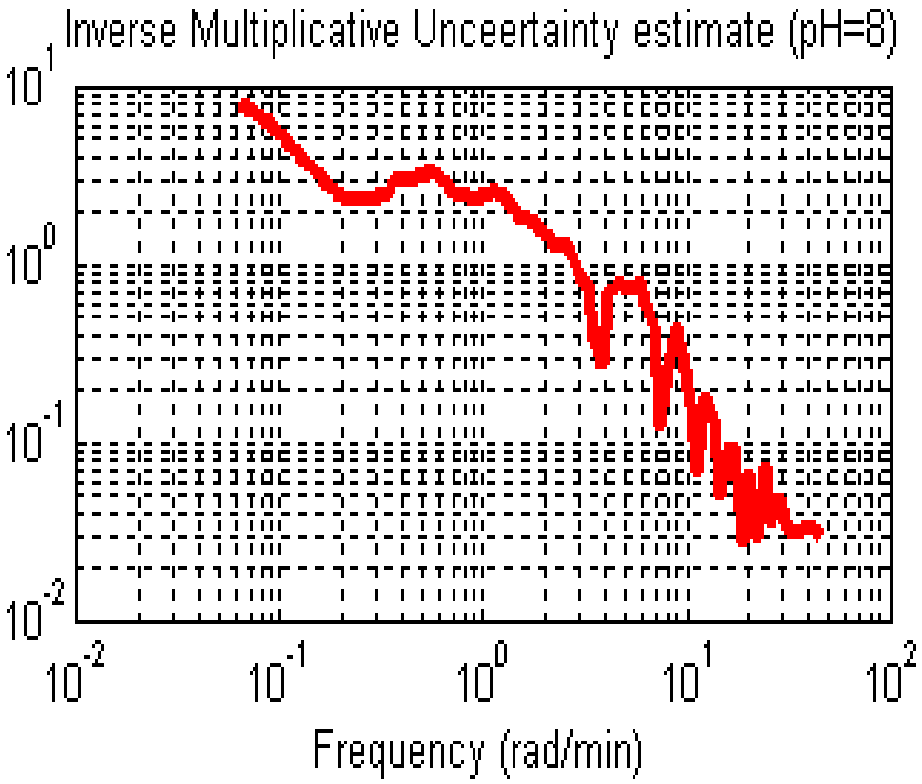

Figure 6, Inverse multiplicative uncertainty estimate for the model at pH = 8, showing an effective bound on the loop bandwidth of 1rad/min (Similar results at pH 6).

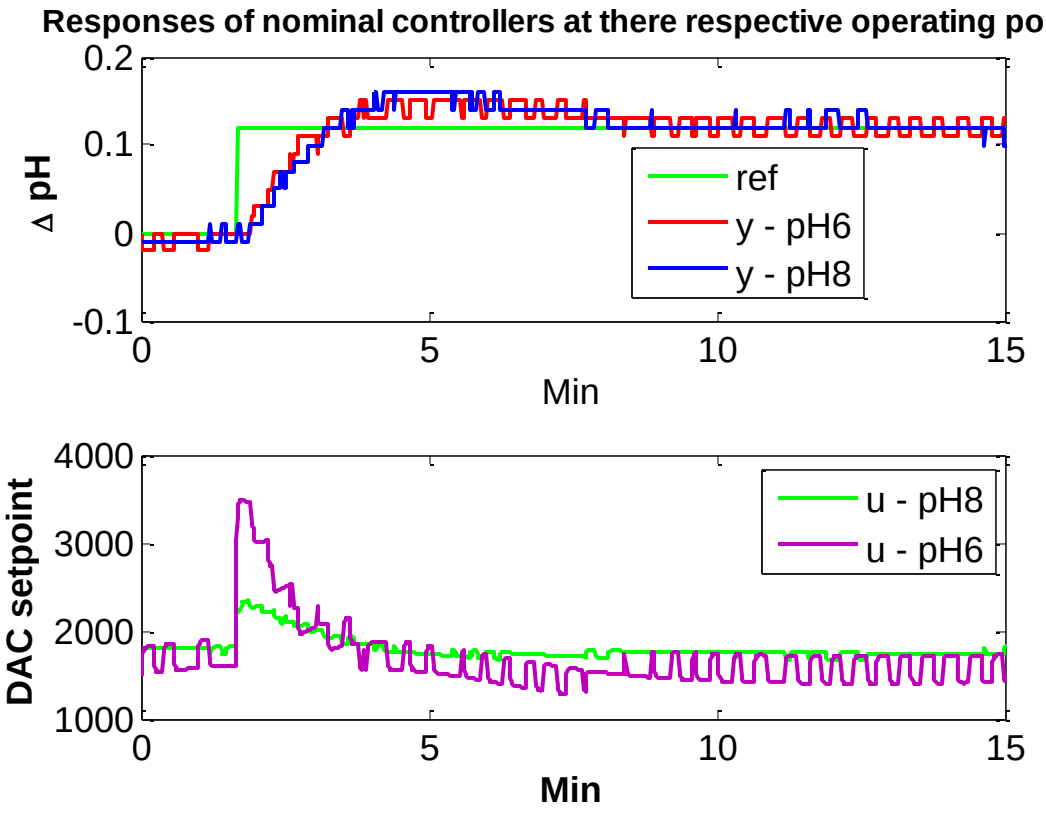

Figure 7a Step reposes of C_6 at pH 6 and C_8 at pH 8

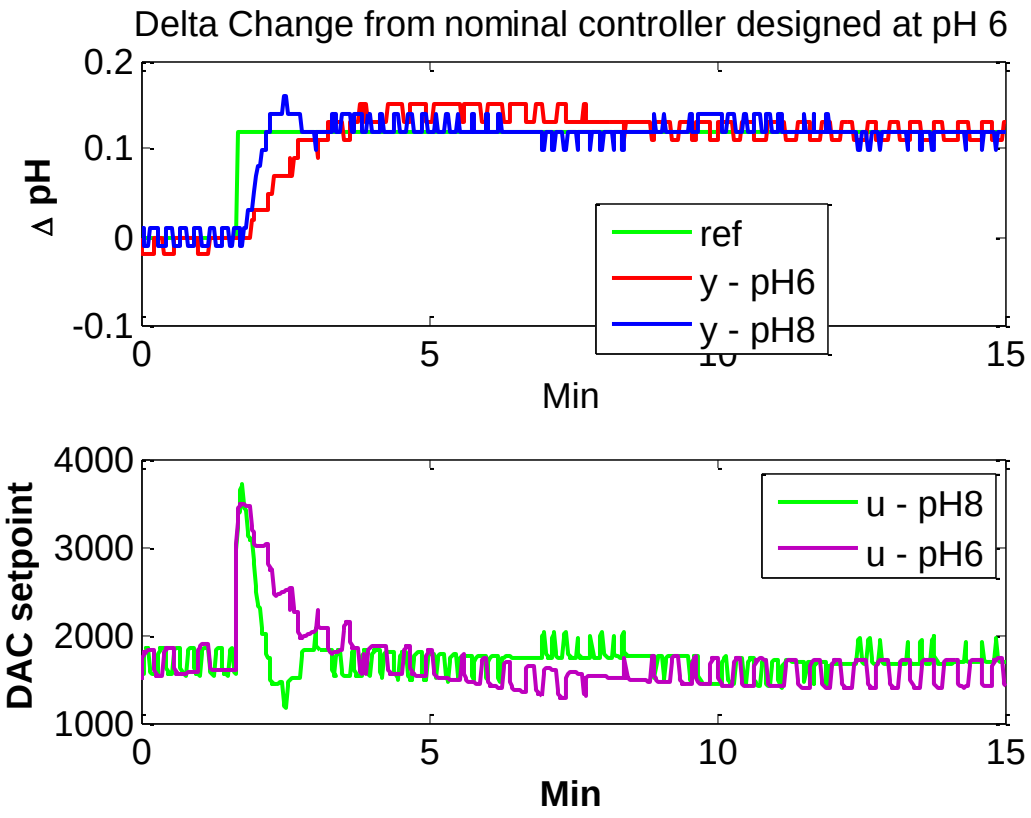

Figure 8b Step responses of C_6 at pH 6 and 8

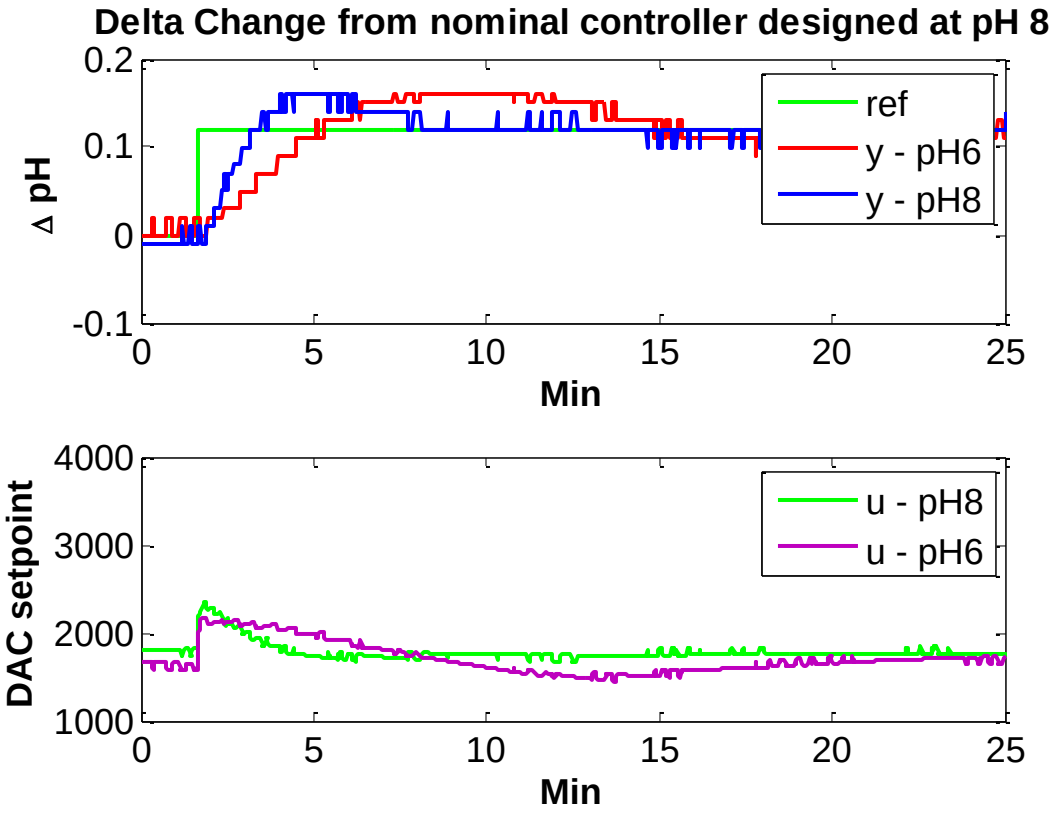

Figure 8c Step responses of C_8 at pH 6 and 8

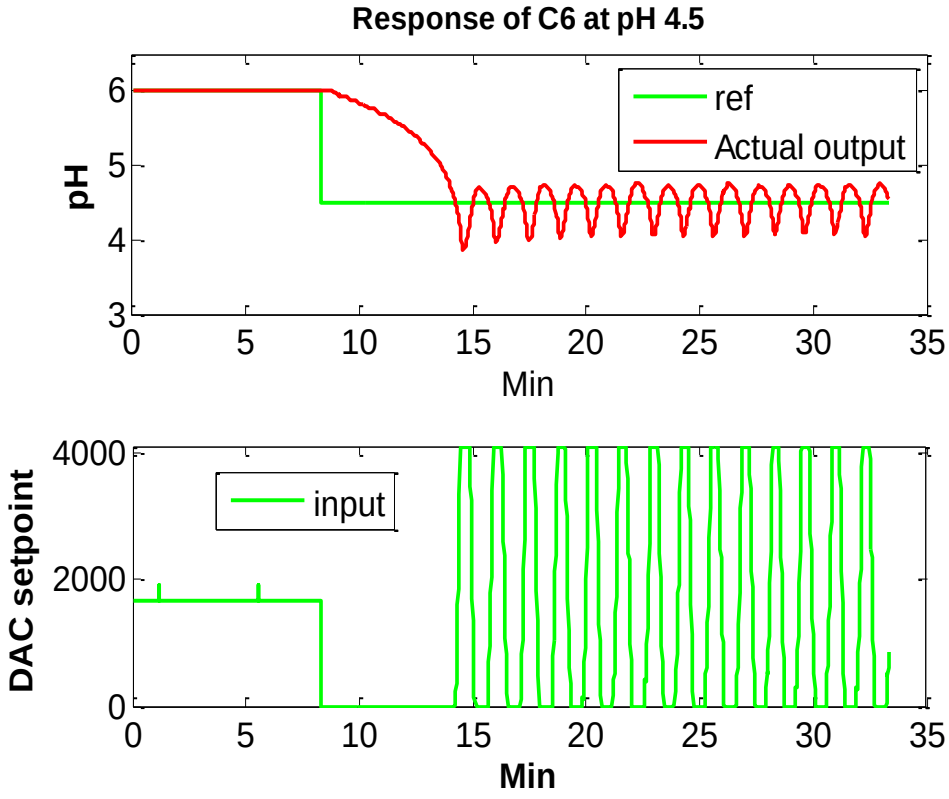

Figure 9 Step response of C_6 at pH 4.5

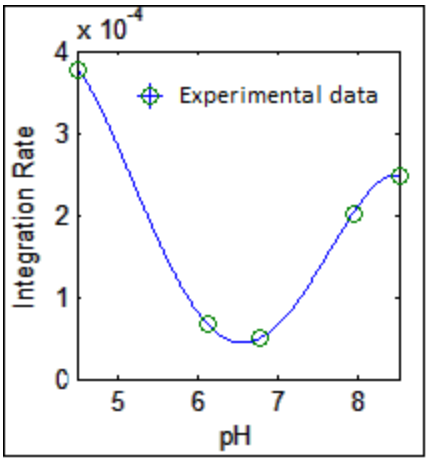

Figure 10 Integration rates as a function of pH for all data

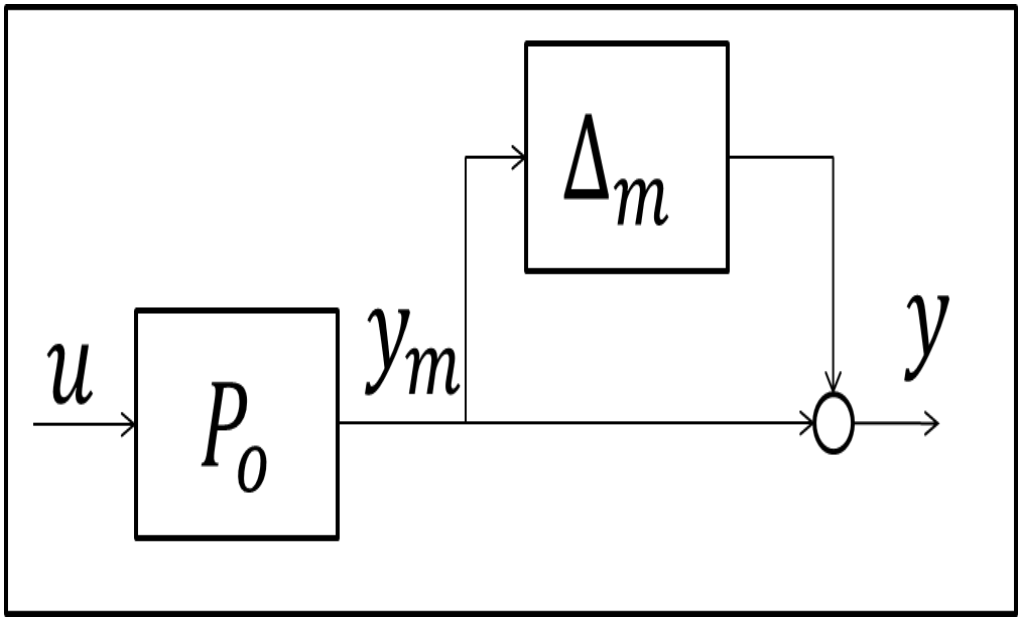

Figure A1:1: Block diagram of multiplicative uncertainty at the output

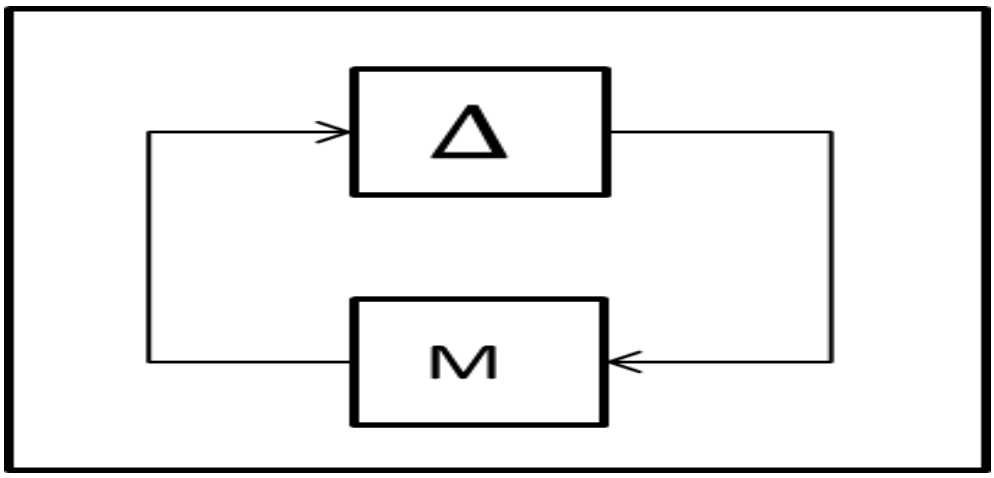

Figure A1:2: Block diagram of general feedback system

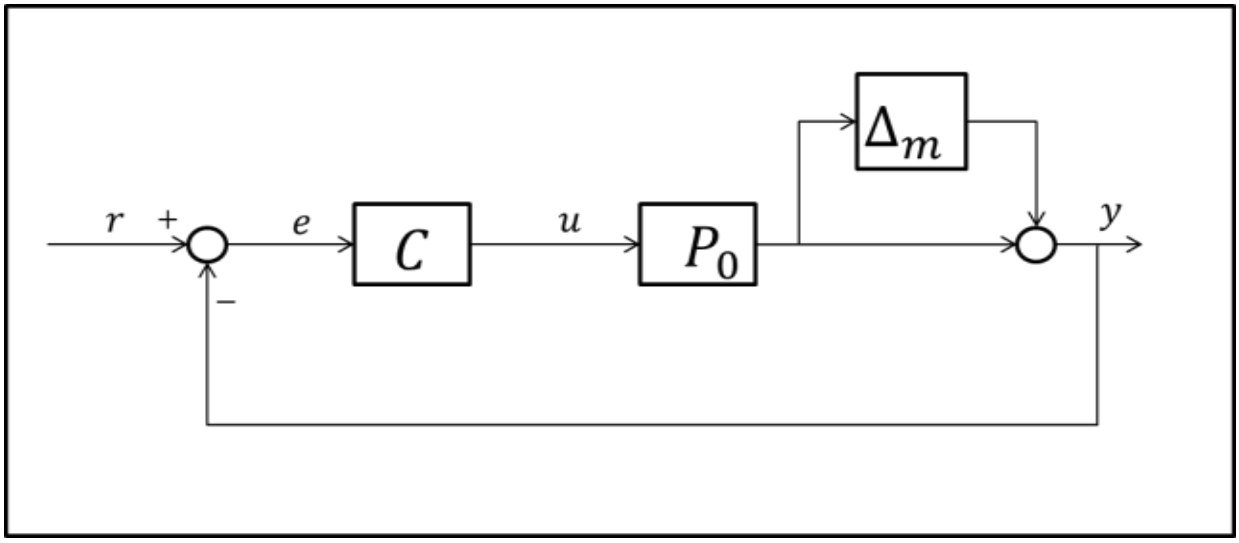

Figure A1:3: Block diagram of feedback system with multiplicative uncertainty

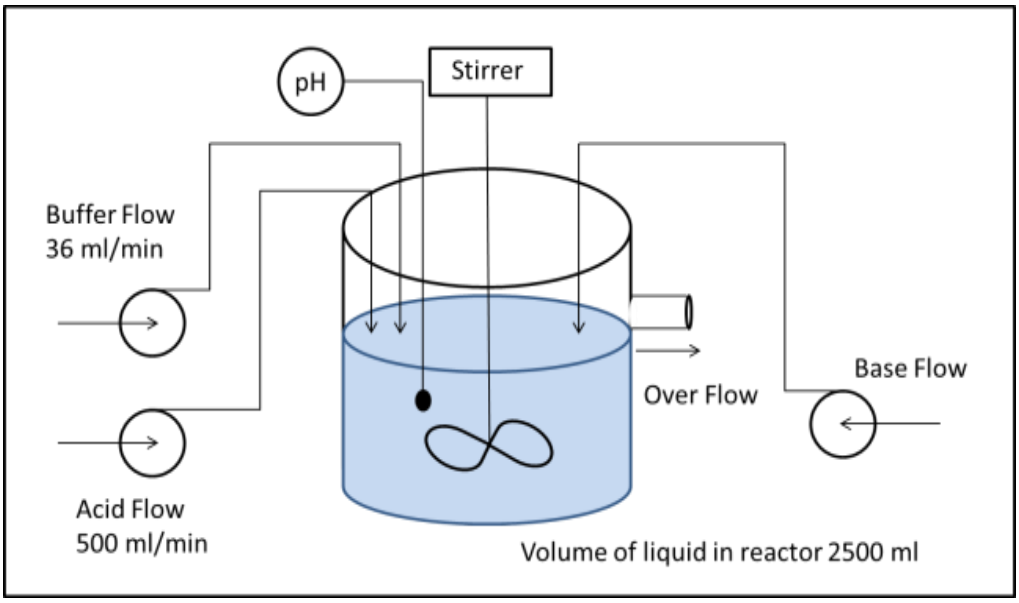

Figure A2:1: Schematic diagram of pH neutralization process

Tables

$Pm = \frac{K}{\tau s + 1}$		
	K	τ
Pm_6	1.5042×10^{-2}	2.6
Pm_8	1.014×10^{-1}	2.372

Table 1: Transfer functions of linearized process models

$P = \frac{K(\tau_1 s + 1)}{s(\tau_2 s + 1)} e^{-T_d s}$				
	K	T_d	τ_1	τ_2
P_6	6.69×10^{-5}	0.367	2.65	2.8
P_7	4.964×10^{-5}	0.217	0	0.0625
P_8	2.02×10^{-4}	0.183	0	0.124

Table 2: Transfer functions of identified process models

Symbol	Values		Symbol	Values		Symbol	Values		Symbol	Values
K_{a1}	4.47×10^{-7}		V	2500 ml		W_{a1}	3×10^{-3}M		W_{b1}	0M
K_{a2}	5.62×10^{-11}		q_1	540 ml/min		W_{a2}	-0.03M		W_{b2}	0.03M
pK_1	6.349692		q_2	36 ml/min		W_{a3}	-3.05×10^{-3}M		W_{b3}	5.0×10^{-5}M
pK_2	10.25026		q_3	510 ml/min		W_{a4}	-4.32×10^{-4}M		W_{b4}	5.38×10^{-4}M

Table 3: Nominal Operating Conditions

Nomenclature

Term	Description
Nominal model(P_0)	Process model that is sued for the controller design and uncertainty characterization
FFT	Fast Fourier transform
ω	Frequency in rad/min
Complementary Sensitivity (T)	Transfer function between reference and output. $T = \frac{PC}{1+PC}$, where P is process model and C is controller transfer function.
Δ_m	Multiplicative uncertainty
$\lvert\Delta_m(j\omega)\rvert$	Magnitude of frequency response of multiplicative uncertainty at frequency ω
Bandwidth	Frequency at which complementary sensitivity (T) crosses 0.707 magnitude. Approximately equal to 1/(Closed-loop time constant)
PID controller structure	$K_c(1 + \frac{1}{T_i S} + T_d S)$ K_c is proportional gain, T_i integral time constant and T_d is derivative time constant.